C. R. Physique 3 (2002) 501–508

Physique statistique, thermodynamique/*Statistical physics, thermodynamics*
(Atomes, molécules/*Atoms, molecules*)

DOSSIER

PHOTONIQUE MOLECULAIRE : MATÉRIAUX, PHYSIQUE ET COMPOSANTS

MOLECULAR PHOTONICS: MATERIALS, PHYSICS AND DEVICES

Single photon emission from a single molecule

François Treussart, Romain Alléaume, Véronique Le Floc'h, Jean-François Roch *

Laboratoire de photonique quantique et moléculaire (UMR 8537 du CNRS et de l'École normale supérieure de Cachan), ENS Cachan, 61, avenue du Président Wilson, 94235 Cachan cedex, France

Accepted 1 March 2002

Note presented by Guy Laval.

Abstract Photon emission from a single molecule at room temperature exhibits nonclassical features. Continuous wave fluorescence excitation provides antibunching in the emitted photons sequence as a signature of the property to only emit one photon at a time. A short pulsed excitation can then produce single photons on demand, with an overall quantum efficiency up to 4.5% in our experimental setup. Direct measurement of the Mandel parameter $Q(T)$ for an observation period of duration T follows a subpoissonian statistics on short time scale and superpoissonian statistics on longer time scale. The latter is attributed to blinking in the fluorescence due to the occurence of a metastable molecular triplet state. ***To cite this article: F. Treussart et al., C. R. Physique 3 (2002) 501–508.*** © 2002 Académie des sciences/Éditions scientifiques et médicales Elsevier SAS

single molecule spectroscopy / nonclassical electromagnetic field state / quantum cryptography

L'émission de photons uniques par une molécule individuelle

Résumé L'émission de photons par une molécule unique présente des caractéristiques non classiques. Lorsque l'on excite sa fluorescence avec un laser continu, il apparaît un phénomène de dégroupement des photons, preuve qu'ils sont émis un à un. L'excitation par des impulsions brèves permet ensuite de produire des photons à la demande, avec une efficacité globale de 4,5% dans notre dispositif expérimental. La mesure directe du paramètre de Mandel $Q(T)$, pour une durée d'observation T, met en évidence des fluctuations d'intensité dont la statistique est subpoissonnienne aux échelles de temps court, et superpoissonnienne sur des échelles de temps plus long. Nous attribuons ce dernier effet au scintillement de la fluorescence qu'entraîne la présence d'un état triplet métastable. ***Pour citer cet article : F. Treussart et al., C. R. Physique 3 (2002) 501–508.*** © 2002 Académie des sciences/Éditions scientifiques et médicales Elsevier SAS

détection de molécules uniques / état non classique du champ électromagnétique / cryptographie quantique

* Correspondence and reprints.
E-mail address: roch@physique.ens-cachan.fr (J.-F. Roch).

S1631-0705(02)01331-2/FLA

1. Introduction

During the past few years the realization of a triggered Single Photon Source (SPS) has attracted much interest for applications in quantum cryptography [1]. A first category of SPS rely on optically [2–5] pumped semiconductor nanostructures. A recent breakthrough happened followed from the demonstration of an electrically pumped SPS [6]. However, the collection efficiency of photons is barely higher than a few 10^{-3} in these experiments performed at cryogenic temperatures. A second category of SPS uses the fluorescence of a single chromophore with a quantum efficiency close to 100%, imbedded in a polymer or crystal host. As shown in a remarkable set of experiments, a single molecule at low temperature behaves as a quantum two-level system [7]. The population of the single molecule can then be efficiently transfered from the ground state to the excited state, relying on the technique of adiabatic passage. Using the Stark effect induced by an applied electric field, the molecular transition frequency is swept through resonance with the laser, so that the molecule is coherently driven into its excited state. It will then emit a pure single photon state, as shown by Brunel et al. [8]. However, in this experiment, the single photon production efficiency was limited, to about 70%, due to technical limitations and emission from the background.

At room temperature, which is more convenient for future applications, the excitation scheme relies on the pulse saturated emission of a single 4-level emitter [9,10]. When the pulse duration τ_p is much shorter than the dipole radiative lifetime τ_{rad}, such a single emitter can then emit only a single photon per excitation pulse. The first room temperature molecular based SPS, realized by Lounis and Moerner [11], relied on the emission of a single terrylene molecule imbedded in a *p*-terphenyl thin microcrystal flake. This system has a high photostability even at room temperature [12,13], since the dye molecules imbedded in the crystal matrix are shielded from exposure to atmospheric oxygen which is the main cause of photobleaching. In the experiment of [11], the signal to background ratio was limited to about 5–10 by crystal absorption and scattering by defects. However, such rather low signal to background ratio is responsible for multiple photons detection events which corresponds to a clear deviation from the perfect SPS. This ratio can be improved by replacing the crystal with a thin polymer host matrix. This was done either with a single molecule [14,15], or with a single NV colored center in diamond nanocrystals [16]. The later system has the advantage of being perfectly photostable at room temperature [17–19].

As we will present in this article, the molecule/polymer system allowed us to observe two non-classical features in the fluorescence of a single emitter, namely antibunching and subpoissonian intensity fluctuations.

2. Experimental setup

Fluorescence from a single molecule is excited and collected by the standard technique of scanning confocal optical microscopy [20]. As shown on Fig. 1, excitation light is reflected by the dichroic mirror of an inverted microscope, and then focused by an oil-immersion objective ($\times 60$, NA $= 1.4$). Light emitted by the sample is collected by the same objective and then focused into a 30 µm diameter pinhole. After recollimation, a holographic notch filter removes the residual pump light. A Hanbury Brown and Twiss (HBT) type of setup is then used to split the beam and detect single photons on two identical avalanche photodiodes. Glass filters are placed onto each arm to suppress parasitic crosstalk between the two photodiodes [21].

3. Results

3.1. CW excitation and antibunching

In order to identify single molecule emission from our sample, we first conducted CW excitation of the chromophore using the 514 nm line of the Ar^+ ion laser [14]. In that case, samples were made of terrylene molecules dispersed at a concentration of about one molecule per 10 µm^2 into a 30 nm thick PMMA

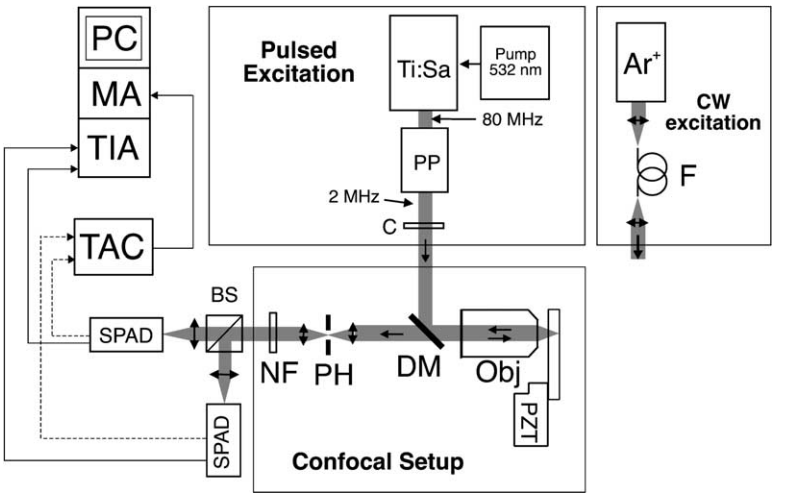

Figure 1. Fluorescence excitation and detection setup relying on a confocal optical microscope. PZT: x, y, z piezo translation stage; Obj: $\times 60$, NA $= 1.4$ objective; DM: dichroic mirror; NF: notch filter. CW excitation is made with a Ar^+ ion laser spatially filtered using a singlemode optical fiber (F). Pulse excitation is achieved by a titanium-dopped-sapphire femtosecond laser (Ti:Sa); PP: pulse picker; C: single-path propagation in a doubling crystal ($LiIO_3$); BS: non-polarizing beamsplitter; SPADs: single-photon counting avalanche photodiodes; TAC: time-to-amplitude converter; TIA: time interval analyser; MA: multichannel analyser; PC: computer.

layer spin-coated onto a cover-glass plate. The time interval between two consecutively detected photons is converted into a voltage with a start–stop protocol using a time-to-amplitude converter set on a full scale of 100 ns. This voltage feeds a multichannel analyzer which builds the time interval histogram $c(\tau)$ (Fig. 1). The width of each channel is $\delta t = 0.19$ ns. In the case of short interphoton times considered here, Fleury et al. [13] proved experimentally that a very good approximation of the intensity autocorrelation function

$$g^{(2)}(\tau) \equiv \frac{\langle I(t)I(t+\tau)\rangle}{\langle I(t)\rangle^2}$$

comes directly from the time interval histogram $c(\tau)$, as predicted by Reynaud [22] in the limits of short timescales and low detection efficiency.

Fig. 2 shows a record of $c(\tau)$ from an isolated emitter. This plot has two scale representations: the right side is the raw coincidence count for an integration interval $T = 100.4$ s and the left scale is the corresponding normalized count $C_N(\tau) \equiv c(\tau)/(R_1 R_2 \delta t T)$, with reference to coincidence counts of

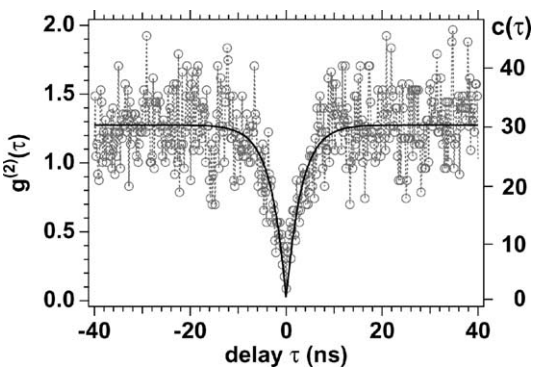

Figure 2. Raw coincidence counts $c(\tau)$ integrated over $T = 100.4$ s (right scale), and $g^{(2)}(\tau)$ (left scale), showing antibunching in the fluorescence of a single terrylene molecule embedded in a thin film of PMMA. The minimum value at $\tau = 0$ is $g^{(2)}(0) = 0.09$.

a poissonian source with counting rates $R_1 = 38 \cdot 10^3$ counts/s and $R_2 = 31 \cdot 10^3$ counts/s measured on each detector for the same integration interval T [19]. The measured signal to background ratio ranges from 15 to 20. The probability that a background photon triggers a coincidence with a photon coming either from the molecule or from the background is therefore very low. It follows that $C_N(\tau)$ can then be directly identified with the correlation function $g^{(2)}(\tau)$. We clearly observed that $g^{(2)}(\tau)$ is almost equal to 0 at $\tau = 0$: two fluorescence photons cannot be detected within an arbitrarily short time interval. This antibunching in the fluorescence of the emitter is due to the finite radiative lifetime of the molecular dipole and is a clear proof that we indeed observe the spontaneous emission of a single molecule. An exponential fit to $g^{(2)}(\tau)$ yields a lifetime $\tau_{rad} = 3.2$ ns, compatible with previously reported value of 3.8 ns for terrylene [11]. Note that for $|\tau| \gg \tau_{rad}$ in Fig. 2, the limit reached by $g^{(2)}(\tau)$ is above unity. As first observed in [23], such a clear signature photon bunching results from molecular intersystem crossing, reflecting a significant transition rate from the excited singlet state to the triplet state [24]. A quantitative analysis suggests that this transition rate is affected by the matrix molecular host [13,14].

3.2. Pulsed excitation and on-demand triggering of single-photon emission

In the case of pulsed excitation, terrylene was replaced by the cyanine dye $DiIC_{18}(3)$. This dye is more suited for future developments which require a control of the excited state dipole orientation. With the selected cyanine dye, such a control can be obtained using for instance Langmuir Blodgett monolayer films. The cyanines are non-resonantly excited at 532 nm, with femtosecond pulses generated by a titanium-dopped-sapphire (Ti:Sa) laser and frequency doubled by single pass propagation into a $LiIO_3$ crystal. The repetition rate, initially at 82 MHz, is divided by a pulsepicker (Fig. 1). The energy per pulse E_p is adjusted by an electro-optic modulator. The pulse duration is about $\tau_p \approx 100$ fs.

In order to rapidly identify single molecule emission, we first measure the intensity autocorrelation function of the fluorescence light with the same start–stop method as the one used for CW excitation. When we address a single emitter, antibunching is observed and characterized by almost no coincidence event at $\tau = 0$ time delay. This is due to the fact that a single photon cannot be simultaneously detected on both sides of a beamsplitter [25]. The histogram shows also a peak pattern at the pulse repetition period τ_{rep}. As explained in [8], the ratios of the lateral peak areas to the central zero delay peak, allow one to infer the probabilities $P_S(n)$ for the source (S), to deliver $n = 0, 1, 2$ photocounts per excitation pulse. Note that two photons counts are due to deviation from the ideal SPS emission. Nevertheless, this technique can hardly be used to extract the intensity fluctuations on timescales longer than a single pulse. We have therefore chosen to record each photodetection event with a two-channel Time Interval Analyser (TIA, see Fig. 1) computer board (GuideTech, Model GT653).

3.2.1. *Pumping of the dye at saturation*

When a single molecule is spotted, we apply the excitation energy ramp $E_p(t)$ shown in the inset of Fig. 3, and simulteaneously record every photocount times. Since each detection channel has a deadtime of 250 ns, the excitation repetition rate was chosen to be 2 MHz. With this progressive excitation method, we achieved higher photostability than by shining upfront the full pump power onto the molecule. This interesting behaviour is currently under study. Fig. 3 displays the fluorescence counting rate R versus E_p. The large intensity fluctuations are due to triplet state excursion of the molecule. If this state is not taken into account, the molecular energy levels can be modelled by a simple 2-level system, assuming a very fast non-radiative relaxation between the two higher and the two lower energy states. The excited state population σ at the time τ_p after the pulse arrival is then

$$\sigma = \frac{E_p/E_{sat}}{1 + E_p/E_{sat}} \left[1 - e^{-\frac{\tau_p}{\tau_{rad}}\left(1+\frac{E_p}{E_{sat}}\right)}\right], \tag{1}$$

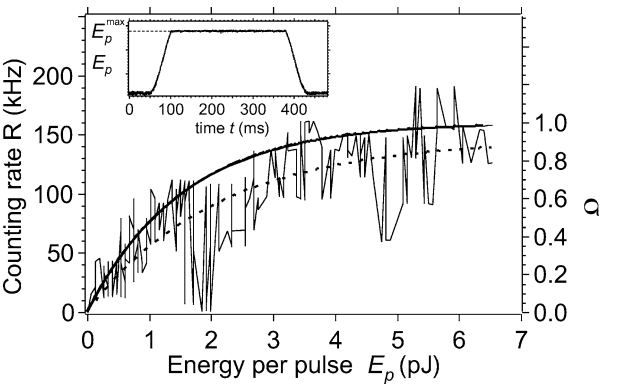

Figure 3. Photon counting rate R versus energy per pulse E_p, for a single cyanine molecule ($\mathrm{DiIC_{18}(3)}$ in a 30 nm thick PMMA thin film). The inset shows the excitation ramp $E_\mathrm{p}(t)$, with $E_\mathrm{p}^{\max} = 13$ pJ in this case. The record of the saturation curve was limited by the photobleaching of the molecule. The dashed curve is a fit of the raw data according to Eq. (1) and the solid line is a fit after correction of triplet state excursion. The right scale shows an estimate of the excited state population σ.

where $\tau_\mathrm{rad} \approx 2.8$ ns for the cyanine considered. The data $R(E_\mathrm{p})$ are fitted by the function $R = R_0 \times \sigma$ in a two steps procedure. After a first fit of the raw data, all the points below this fit are attributed to triplet state excursion and are then removed. The fit of the remaining set of data yields $R_0 = 160 \cdot 10^3$ counts/s and $E_\mathrm{sat} = 5.6 \cdot 10^{-5}$ pJ.

In order to optimize the number of emitted photons and avoid rapid photobleaching, we then set $E_\mathrm{p}^{\max}$ to 5.6 pJ. Such a value would correspond to an estimated excited state population $\sigma = 97\%$, for the molecule studied in Fig. 3. During the constant maximum pumping energy period of the excitation ramp, 10^4 detection events are typically recorded before the occurence of photobleaching. Thanks to the high stability of the frequency of the pulsed femtosecond laser, the set of photocount records is afterwards synchronized to an excitation timebase. This procedure consists in minimizing the time delays between the detection and excitation events over the whole set of measurements, with the laser pulse excitation period and a constant emitter-to-detector propagation delay as the two free parameters. We finally end-up with a table which includes, for each excitation pulse i, the number of photocounts $n_i = 0, 1, 2$ and the time delay δt_i between the excitation pulse and the recording of the detected photon.

The data considered hereafter corresponds to a molecular source (S) which survived during 319 769 periods (about 160 ms) at constant saturation excitation power, yielding 14 928 recorded photons. This includes 14 896 single photon events and 16 two-photons events. We deduced for the single photon source (S) the probability $P_\mathrm{S}(1) = 0.0466$ of emitting a one-photon pulse, and a probability $P_\mathrm{S}(2) = 5.0 \cdot 10^{-5}$ of emitting a two-photon pulse. The mean number of detected photon per excitation pulse is $\overline{n}_\mathrm{S} = 0.0467$. The real source is considered as the superposition of an attenuated ideal SPS with an overall quantum efficiency η, and a coherent source simulating the background which adds a mean number of detected photon per pulse γ. From the measured values of $P_\mathrm{S}(1)$ and $P_\mathrm{S}(2)$, we infer $\eta \approx 0.0445$ and $\gamma \approx 2.2 \cdot 10^{-3}$. This leads to a signal-to-background ratio of about 20, similar to the one previously achieved under CW excitation.

We compared experimentally our SPS to an experimental reference source (R) made of attenuated pump laser pulses, with approximately the same mean number of detected photons per pulse. We checked that this source is a very good approximation of a coherent source. We measured that the ratio of two-photon events for the reference $P_\mathrm{R}(2)$ and the SPS source $P_\mathrm{S}(2)$ is $P_\mathrm{S}(2)/P_\mathrm{R}(2) \approx 0.10$. This means that the number of two photons pulses is 10 times smaller for our SPS than for the reference poissonian source (R).

3.2.2. *Intensity fluctuations on a wide range of observation timescale*

In order to quantify the fluctuations of the number of photons n detected per pulse, and compare the SPS to an equivalent coherent light source, one can use the Mandel parameter $Q \equiv \langle (\Delta n)^2 \rangle / \langle n \rangle - 1$ [26]. Poissonian photocounts statistics yields $Q = 0$ whereas subpoissonian and superpoissonian statistics corresponds respectively to the negative and positive Q's. From our measurement of the photocount times, we calculated $Q = -0.0445$. Let us point out that due to the photodetection deadtime, the triggered

reference source (R) also yields a subpoissonian counting statistics. More precisely, for the coherent source (C) giving the same mean number $\overline{n}_C$ of photons per pulse than our SPS, one predicts a value $Q_C = -\overline{n}_C/2 = -0.0231$. This is confirmed by our measurements on the reference source. The fluctuations of the number of detected photons per pulse coming out of our SPS clearly evidences a departure from the reference coherent source. Albeit still limited by the quantum efficiency η, this direct measurement of the Mandel parameter is already larger by more than one order of magnitude than previous measurements realized in experiments with either a single atom [27] or a single trapped ion [28]. For a solid state SPS like ours, any improvement achieved in the light collection efficiency would therefore yield higher values of the subpoissonian character.

Nevertheless, the triplet state in the molecular energy diagram also affects the intensity fluctuations on timescales longer than a single pulse. As the leak in this dark triplet state induces correlations between consecutive pulses, the measurement of the fluctuations of the number n_i of detected photons per pulse is not sufficient for a complete characterization of the molecular based SPS noise properties. The analysis of the fluctuations of the variable n_i can however be generalized to the variable $N(T)$, which is the total number of photocounts recorded during an observation time interval T. Using the time dependent Mandel parameter [29] $Q(T) \equiv \langle(\Delta N)^2\rangle_T / \langle N\rangle_T - 1$, we also define a Mandel parameter $Q_s(T)$ for the number of photons *emitted* by the source in the same period of time T. In the case of an ideal SPS, one simply has $Q = \eta \times Q_s$ [30]. Since $Q_s = -1$ for ideal single photon emission, $Q(T) = -\eta$ for any value of T.

Fig. 4 shows that we did observe subpoissonian intensity fluctuations on timescales from $T = 1 \times \tau_{rep}$ to $T \approx 8 \times \tau_{rep}$, with the minimum value $Q(\tau_{rep}) = -0.0445$ achieved on a single pulse timescale as explained above. When we consider the number of detected photons on timescales larger than 10^{-5} s, the intensity fluctuations exhibit a superpoissonnian behaviour ($Q(T) > 0$) as shown on the inset of Fig. 4. This is a direct consequence of bunching in the photon emission due to the triplet state, as previously observed with $g^{(2)}$ measurement (Fig. 2).

We developped a simple model to account for these measurements, relying on the intermittency of the SPS emission. In this model, the molecule is either available for fluorescence and is said to be in a ON state, or it is in its triplet OFF state and does not fluoresce. Let us note p, the probability per unit of time to make a ON $\rightarrow$ OFF transition, and $q = 1/\tau_T$ the one to make the reverse OFF $\rightarrow$ ON transition, where τ_T is the lifetime of the triplet state. Note that $p\tau_{rep} = \mathcal{P}_{ISC}$ is the intersystem crossing probability per excitation pulse. From measured values at the single molecule level with $DiIC_{18}(3)$ cyanine dye [31], $p\tau_{rep} \approx 10^{-4} \ll 1$ and $q\tau_{rep} \approx 2.5 \cdot 10^{-3} \ll 1$. In this limiting case, the Mandel parameter of the source is

$$Q_s(k\tau_{rep}) = \frac{2 \times \mathcal{P}_{ISC}}{\beta^2}\left\{1 - \frac{1}{k\beta}\left[1 - (1-\beta)^k\right]\right\} - 1 \tag{2}$$

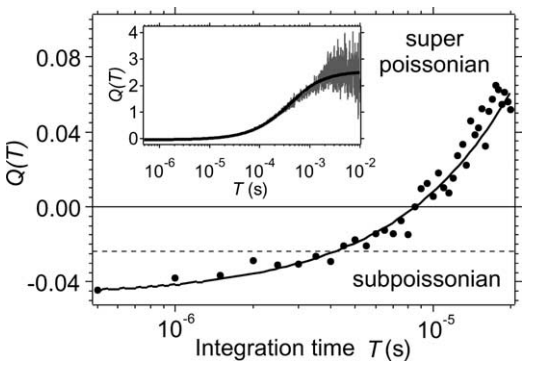

Figure 4. Direct measurements of Mandel parameter $Q(T)$ over 4 orders of magnitude of the recording time T. Dashed line shows $Q(T)$ for the equivalent coherent source (C). Inset shows $Q(T)$ for longer time of observation. The solid curve is a fit to the data by a model accounting for intermittency in the SPS emission. On long timescales, large fluctuations of $Q(T)$ are due to the finite number of available photocounts.

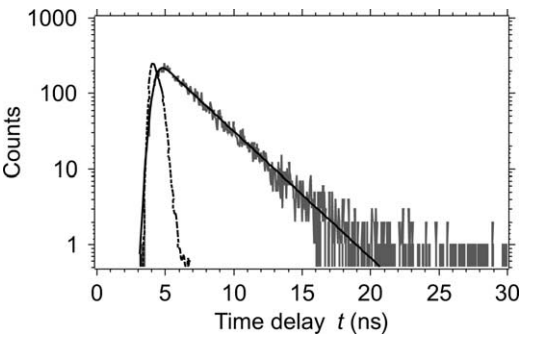

Figure 5. Histogram of time delays t (same molecule as in Section 3.2.1) for the whole set of 14 928 detected photons. The dashed line is the instrument time response function IRF(t). The solid line is a least-square fit to the data by the convolution of a monoexponential decay and the response function IRF(t), yielding a characteristic fluorescence decay time $\tau_{\mathrm{rad}} = 2.6$ ns.

where $\beta \equiv (p+q)\tau_{\mathrm{rep}} = \mathcal{P}_{\mathrm{ISC}} + \tau_{\mathrm{rep}}/\tau_{\mathrm{T}}$. The Mandel parameter of the detected photon counts is then $Q(T) = \eta \times Q_{\mathrm{s}}(T)$. As shown on Fig. 4, our data for $Q(T)$ are well fitted by Eq. (2) over more than 4 orders of magnitude, with $\eta = 0.0445$ (measured) and the free parameters p and q. The fit yields $p\tau_{\mathrm{rep}} \approx 2 \cdot 10^{-4}$ and $\tau_{\mathrm{T}} \approx 250$ µs, values which are in good agreement with a previous measurement of these parameters [31].

3.3. Time-resolved single-molecule photophysical dynamics

Our time resolved photon counting measurements also allows one to track the molecular dynamics at all time scales. For instance, one can directly extract from the set of photocounts the single-molecule fluorescence lifetime τ_{rad}. Fig. 5 shows the histogram of time delays δt_i between the record of the photon emission and the excitation pulse, for the whole set of 14 928 detected photons from the same molecule as the one considered in Fig. 4. These delays have to be corrected from the instrument time response fonction IRF(δt). A gaussian function is taken here as a first crude approximation of this response function. The resulting signal is the convolution of the molecular fluorescence monoexponential decay by the instrument response function $\exp(-\delta t/\tau_{\mathrm{rad}}) \cdot \mathrm{IRF}(\delta t)$. The least mean square fit of our data by this convolution function yields a fluorescence lifetime $\tau_{\mathrm{rad}} = 2.6$ ns. This value is also in good agreement with previously reported measurements for a very similar cyanine [32].

Let us point out that this measurement of τ_{rad} is only a mean value over the whole emission period, and one may imagine some fluctuations of the fluorescence lifetime due for instance to local field fluctuations in the polymer matrix host. If, in principle, time-resolved fluorescence lifetime measurements could be made on a subset of detection events, a simple least mean square fit analysis does not give stable results for a number of events smaller than $\approx 2 \cdot 10^4$ [33]. A more specific analysis, using for instance a maximum likelihood estimator [33], should be applied to extract accurate lifetime values from subsets of only 10^3 events.

4. Conclusions

We have demonstrated an efficient triggered single-photon/single-molecule source operating at room temperature and have investigated its noise properties. Non-classical photocount statistics is clearly observed. We now plan to couple the molecular dipole to a single mode of microcavity in order to define more precisely the polarization and spectral properties of the emitted photons. To achieve this goal, control of the molecular dipole orientation is required, with the Langmuir Blodgett monolayer deposition technique as an interesting candidate. Single molecule fluorescence is also a powerful tool to study the radiation of a single dipole next to an interface, and to measure the modifications of radiative lifetime and the far-field fluorescence radiation pattern due to the electromagnetic boundary conditions [34–36], now at the single-molecule level.

The results presented here, show that realizing a molecular single photon source suited for applications, still remains a difficult experimental challenge. Nevertheless, recent advances in molecular scale electronics

[37,38] may allow one to electrically control the fluorescence of a single-molecule. Even if there is obviously a long road ahead, this would pave the way for 'molecular optoelectronics' at the single-molecule level.

Acknowledgements. We are grateful to J.-M. Courty, C. Grossman and L.T. Xiao for their contribution at some point in the experiment. We thank J. Zyss and P. Grangier for their support and many valuable discussions. The experimental setup was built thanks to the great technical assistance of A. Clouqueur, J.-P. Madrange and C. Ollier. This work was supported by the Ministère de la Recherche (ACI Jeunes Chercheurs and ACI Nanostructures) and by a France Télécom R&D grant (CTI Télécom Quantique).

References

[1] N. Gisin, G. Ribordy, W. Tittel, H. Zbinden, Rev. Mod. Phys. (2001), submitted, quant-ph/01011098.
[2] J. Kim, O. Benson, H. Kan, Y. Yamamoto, Nature 397 (1999) 500.
[3] P. Michler, A. Kiraz, C. Becher, W. Schoenfeld, P. Petroff, L. Shang, E. Hu, A. Imamoğlu, Science 290 (2000) 2282.
[4] C. Santori, M. Pelton, G. Solomon, Y. Dale, Y. Yamamoto, Phys. Rev. Lett. 86 (2001) 1502.
[5] E. Moreau, I. Robert, J.-M. Gérard, I. Abram, L. Manin, V. Thierry-Mieg, Appl. Phys. Lett. 79 (2001) 2865.
[6] Z. Yuan, B.E. Kardynal, R. Stevenson, A. Shields, C. Lobo, K. Cooper, N. Beattie, D. Ritchie, M. Pepper, Science 295 (2002) 102.
[7] P. Tamarat, A. Maali, B. Lounis, M. Orrit, J. Phys. Chem. A 104 (2000) 1.
[8] C. Brunel, B. Lounis, P. Tamarat, M. Orrit, Phys. Rev. Lett. 83 (1999) 2722.
[9] F.D. Martini, G.D. Giuseppe, M. Marrocco, Phys. Rev. Lett. 76 (1996) 900.
[10] R. Brouri, A. Beveratos, J.-P. Poizat, P. Grangier, Phys. Rev. A 62 (2000) 063817.
[11] B. Lounis, W.E. Moerner, Nature 407 (2000) 491.
[12] L. Fleury, B. Sick, G. Zumofen, B. Hecht, U. Wild, Molec. Phys. 95 (1998) 1333.
[13] L. Fleury, J.-M. Segura, G. Zumofen, B. Hecht, U. Wild, Phys. Rev. Lett. 84 (2000) 1148.
[14] F. Treussart, A. Clouqueur, C. Grossman, J.-F. Roch, Opt. Lett. 26 (2001) 1504.
[15] F. Treussart, R. Alléaume, V.L. Floc'h, L. Xiao, J.-M. Courty, J.-F. Roch, quant-ph/0202130, 2002.
[16] A. Beveratos, S. Kühn, R. Brouri, T. Gacoin, J.-P. Poizat, P. Grangier, Eur. Phys. J. D 18 (2002) 191.
[17] A. Gruber, A. Dräbenstedt, C. Tietz, L. Fleury, J. Wrachtrup, C.V. Borczyskowsky, Science 276 (1997) 2012.
[18] C. Kurtsiefer, S. Mayer, P. Zarda, H. Weinfurter, Phys. Rev. Lett. 85 (2000) 290.
[19] R. Brouri, A. Beveratos, J.-P. Poizat, P. Grangier, Opt. Lett. 25 (2000) 1294.
[20] S. Nie, R. Zare, Annu. Rev. Biophys. Biomol. Struct. 26 (1997) 567.
[21] C. Kurtsiefer, P. Zarda, S. Mayer, H. Weinfurter, J. Mod. Opt. (2001), submitted.
[22] S. Reynaud, Ann. Phys. France 8 (1983) 315.
[23] J. Bernard, L. Fleury, H. Talon, M. Orrit, J. Chem. Phys 98 (1993) 850.
[24] J. Lakowicz, Principles of Fluorescence Spectroscopy, Kluwer Academic, 1999.
[25] P. Grangier, G. Roger, A. Aspect, Europhys. Lett. 1 (1986) 173.
[26] R. Loudon, The Quantum Theory of Light, Oxford University Press, 2000.
[27] R. Short, L. Mandel, Phys. Rev. Lett. 51 (1983) 384.
[28] F. Diedrich, H. Walther, Phys. Rev. Lett. 58 (1987) 203.
[29] L. Mandel, Opt. Lett. 4 (1979) 205. In the definition of $Q(T)$, $\langle\rangle_{\mathrm{T}}$ stands for the mean value over sets of measurements lasting T.
[30] J. Abate, H. Kimble, L. Mandel, Phys. Rev. A 14 (1976) 788.
[31] J. Veerman, M. Garcia-Parajo, L. Kuipers, N.V. Hulst, Phys. Rev. Lett. 83 (1999) 2155.
[32] J. Macklin, J. Trautman, T. Harris, L. Brus, Science 272 (1996) 255.
[33] M. Maus, M. Cotlet, J. Hofkens, T. Gensch, F. de Schryver, Anal. Chem. 73 (2001) 2078.
[34] R. Chance, A. Prock, R. Silbey, J. Chem. Phys. 60 (1974) 2744.
[35] R. Chance, A. Miller, A. Prock, R. Silbey, J. Chem. Phys. 63 (1975) 1589.
[36] W. Lukosz, J. Opt. Soc. Am. 69 (1979) 1495.
[37] J. Schön, H. Meng, Z. Bao, Science 294 (2001) 2138.
[38] J. Schön, H. Meng, Z. Bao, Nature 413 (2001) 713.